

# An AGC Reformulation for the Decomposed Security-Constrained ACOPF Problem

Muhammad Waseem, *Student Member, IEEE* and Saeed D. Manshadi, *Member, IEEE*

arXiv:2012.13110v2 [math.OC] 2 Jan 2021

**Abstract**—This paper presents a reformulation for the automatic generation control (AGC) formulation in a decomposed convex relaxation algorithm to find an optimal solution to the AC optimal power flow (AC-OPF) problem which is secure against a large set of contingencies. First, the master problem, which represents the system without contingency constraints, is convexified by applying the second-order cone relaxation approach. Second, the contingencies are filtered for corrective or preventive actions. The contingencies for preventive security check sub-problems are evaluated in a parallel computing process to improve computational efficiency. The AGC is modeled by a set of proposed valid constraints, so the solution obtained in each security check sub-problem is the physical response of the system during a contingency. Third, Benders optimality cuts are generated for the sub-problems with mismatches. The cuts are passed to the master problem to encounter the security constraints. The proposed convex relaxation for the master problem ensures the convergence of the decomposition algorithm. The effectiveness of the presented valid AGC constraints and scalability of the proposed algorithm are illustrated in several case studies.

**Index Terms**—Automatic generation control, AC optimal power flow, contingency analysis, parallel computing, Benders decomposition.

## NOMENCLATURE

### Indices

$e \in \mathcal{E}$	Index of line in the set of lines
$f \in \mathcal{F}$	Index of transformer in the set of transformers
$g \in \mathcal{G}$	Index of generator in the set of generators
$k \in \mathcal{K}$	Index of contingency
$i \in \mathcal{I}$	Index of bus in the set of buses
$i_g$	Index of bus connected to generator

### Variables

$c_g$	Generation cost of generator ( $g$ ) as a function of active power (USD/h)
$p_e^{ij}$	Line $e$ real power from origin bus $i$ to bus $j$
$p_f^{ij}$	Transformer $f$ real power from origin bus $i$ to bus $j$
$p_g$	Generator $g$ real output power
$q_e^{ij}$	Line $e$ reactive power from origin bus $i$ to bus $j$
$q_f^{ij}$	Transformer $f$ reactive power from origin bus $i$ to bus $j$
$q_g$	Generator $g$ reactive output power
$v_i$	Bus $i$ voltage magnitude
$e_i$	Real part of voltage at bus $i$
$f_j$	Imaginary part of voltage at bus $j$
$\Delta_k$	Contingency $k$ scale factor on generator participation factors defining generator real power contingency response

M. Waseem and S. D. Manshadi are with San Diego State University, San Diego, CA 92182 USA e-mail: mwaseem2282@sdsu.edu; smanshadi@sdsu.edu.

$\sigma_{ik}^{P+/-}$	Apparent power mismatch for contingency $k$ in bus $i$ real power positive/negative parts
$\sigma_{ik}^{Q+/-}$	Apparent power mismatch for contingency $k$ in bus $i$ reactive power positive/negative parts
$\sigma_{ek}$	Apparent power mismatch for contingency $k$ in line $e$
$\sigma_{fk}$	Apparent power mismatch for contingency $k$ in transformer $f$

### Parameters

$b_e$	Line $e$ series susceptance
$b_f$	Transformer $f$ susceptance
$b_e^{CH}$	Line $e$ total charging susceptance
$g_e$	Line $e$ series conductance
$p_g$	Generator $g$ real power maximum
$\underline{p}_g$	Generator $g$ real power minimum
$\overline{q}_g$	Generator $g$ reactive power maximum
$\underline{q}_g$	Generator $g$ reactive power minimum
$\overline{R}_e$	Line $e$ apparent current maximum in base case
$\overline{R}_e^K$	Line $e$ apparent current maximum in contingencies
$\overline{s}_f$	Transformer $f$ apparent power maximum in base case
$\overline{s}_f^K$	Transformer $f$ apparent power maximum in contingencies
$\overline{v}_i$	Bus $i$ maximum voltage magnitude in the base case
$\underline{v}_i$	Bus $i$ minimum voltage magnitude in the base case
$\overline{v}_i^K$	Bus $i$ maximum voltage magnitude in contingencies
$\underline{v}_i^K$	Bus $i$ minimum voltage magnitude in contingencies
$\alpha_g$	Participation factor of generator $g$ in real power contingency response
$\delta$	Weight on base case in objective
$b_f^M$	Transformer $f$ magnetizing susceptance
$b_i^{FS}$	Bus $i$ fixed shunt susceptance
$g_f$	Transformer $f$ series conductance
$g_f^M$	Transformer $f$ magnetizing conductance
$g_i^{FS}$	Bus $i$ fixed shunt conductance
$p_i^L$	Bus $i$ constant real power load
$q_i^L$	Bus $i$ constant reactive power load
$\tau_f$	Transformer $f$ tap ratio
$t_m$	Magnitude of complex transformer ratio
$t_r$	Real part of complex transformer ratio
$t_i$	Imaginary part of complex transformer ratio

## I. INTRODUCTION

THE inclination to optimally operate the power system may lead to operating points close to the boundary of the security limits. When severe contingencies occur in a power system leading to instabilities or blackouts, it becomes

necessary to secure the power system using preventive or corrective control actions. The Security assessment is one of the most fundamental elements in power system operation. Its main objective is to ascertain if the power system is secure with respect to contingencies.

An optimal power flow (OPF) problem finds an optimal operating point for an objective function under given constraints. In literature, security-constrained optimal power flow (SCOPF) appears when contingency constraints are considered in an OPF [1]. It considers contingencies involving the disruption of generating stations and transmission lines and the controlling calculations are carried out during power system operation and planning stage. Steady-state security is the capability of the system to function continuously within the rating of the equipment after a contingency has occurred [2]. The SCOPF problem is mainly classified into two classes: corrective and preventive formulations [2], [3]. The corrective formulation reschedules the power flow after the outage has occurred. The corrective SCOPF includes one set of control variables for normal operating conditions and another set of alteration variables for the contingency scenarios. The control variables in post-contingency are allowed to remove the violations caused by contingencies. The corrective model requires additional constraints and variables and many reschedules are required to perform the corrective actions. An iterative approach to solving corrective SCOPF is proposed in [4]. It considers a subset of potential contingencies, a steady-state security analysis, a contingency filtering technique, and checking post-contingency state feasibility. On the other hand, preventive formulation considers normal situation control variables to minimize the cost function. The preventive SCOPF deals with one set of variables to fulfill both normal and contingency circumstances. A dispatch involving security constraints implements preventive control and thus better system security is achieved [3]. The preventive generation rescheduling scheme using trajectory sensitivity analysis is proposed in [5]. An effective AC corrective/preventive contingency dispatch for the security-constrained unit commitment model to minimize the power system operational cost while preserving the system security is presented in [6]. The preventive SCOPF should only be applied when corrective actions are not enough or cannot be applied quickly [7].

The main drawback of traditional SCOPF algorithms is the negligence of stability requirements and problem size because it is challenging to incorporate these in a forthright way [8]. Monte Carlo method is used for post-fault stability assessment and high-density sampling of operating points through time-domain simulations in [9]. A generation rescheduling method to increase the dynamic security of power systems is proposed in [10]. A semi-definite programming relaxation to develop minimum singular value into voltage stability constrained OPF model is studied in [11]. The recognition of critical control violations is very essential because their location in the system is critical for deciding on the installation of additional controls during the planning and the activation of the same controls during operation [12]. The solution of an optimization problem over a relaxed set gives lower bound on the optimal generation cost. However, the solution may risk system security and may

not be feasible [13]. A sparse tableau formulation for node-breaker representations in security-constrained optimal power flow is proposed in [14].

A large power system network involving numerous contingencies results in greater execution time and memory requirements. Thus, algorithms are created to consider the only potentially binding contingencies into the methodology [15]. The number of contingencies can be reduced using screening procedures [16]. The network dimension reduction technique by ignoring the less affected areas of the system is proposed in [17]. Two contingency filtering techniques depending upon the post-contingency violations are proposed in [15]. The ranking procedure chooses contingencies based on a severity index that has a pre-defined threshold limit. A bi-level maximum-minimum optimization model to find the critical contingencies is developed in [7]. A contingency selection procedure based on the contingency explicit ranking is discussed in [18].

The security-constrained optimal power flow problem is a large scale optimization problem. A commonly used technique to solve SCOPF is Benders decomposition, which can take advantage of problem structure [19]. Benders decomposition reduces the complexity of the problem by decomposing the original problem into master and various sub-problems [20]. Benders decomposition is used to solve the optimal power flow master problem in [21]. But the number of decision variables is greater for large power systems. It assumes short-term emergency ratings quite high that could result in voltage collapse or cascading outages before the corrective actions are effective. Benders decomposition is used to decompose the SCOPF problem into sub-problems associated with each contingency [19]. It decomposes the problem into a master and sub-problems, where sub-problems check solution feasibility for the master problem. An optimal solution to the master problem is found, and if the sub-problems are feasible, the master solution is the overall problem solution. Infeasible sub-problems generate cuts for the master problem, and the procedure is repeated until a feasible solution is obtained.

AGC is a speed governing property of a generation unit. It utilizes the power generation capacity to optimally distribute the power during disturbances in an interconnected system while minimizing the real-time generation cost. It offers significant cost savings under load variability and uncertain conditions while constraining the thermal rating limits of tie-lines. The AGC implemented in [22] ignores the tie-line thermal limits. The thermal limits on the tie-line are considered in [23] but AGC is not considered here. Besides, the corrective SCOPF presented in [24] does not consider the AGC response of generation units.

The previous works presented in the literature are facing three main challenges: considering AC power flow constraints, modeling the AGC response, and scalability to tackle large scale problems with a large set of contingencies. For example, the contingency ranking method proposed in [25] is not necessarily computationally efficient for a large network with numerous potential contingencies. Another example is the utilization of Benders decomposition to enhance the scalability in [26] that considered DC power flow constraints, instead of AC power flow constraints. Thus, this paper aims to address

the three main questions: 1) *What is the impact of modeling AGC response of generation units during contingencies?* 2) *What is the impact of full-AC power flow constraints on the SCOPF problem?* 3) *Is it possible to develop a scalable algorithm?* In summary, the main contributions of this paper are listed as follows:

- 1) The AGC response of generations units in each contingency is modeled by introducing a set of valid constraints presenting the AGC response to changes in the system and integrate it with full AC power flow constraints. Thus, the procured solution presented in the security check sub-problem is the physical response of the system in case of contingency.
- 2) The full AC-OPF problem formulation is presented for both master problem and each contingency check sub-problems. The second-order cone relaxation of the master problem is employed to present the master problem in convex form. A tightness measure method is utilized to verify the merit of the employed convex relaxation approach.
- 3) Once the contingencies are filtered to be considered in a preventive or corrective approach, those selected for preventive security check sub-problems are checked in parallel. This presents an improved computationally efficient approach to scale up to check the security of the procured AC-OPF solution in the master problem for a large number of contingencies.
- 4) An application of the Benders decomposition approach is presented, where the merit of the presented convex relaxation for the master problem is illustrated in the convergence of the decomposition algorithm.

## II. PROBLEM FORMULATION

The original problem of SCOPF is presented in two parts which include the base problem and the constraints associated with each contingency. The base case problem formulation is given in (1). The piece-wise objective function is represented by (1a) where  $h_1$  and  $h_2$  are linear function of bus injection mismatches. Base case bounds on voltage, real power, and reactive power are constrained by (1b), (1c), and (1d) respectively. Base case real and reactive power flows into a transmission line at the origin buses are defined by (1e) and (1f) respectively. The real and reactive power flow into a transformer at the origin buses in the base case is represented by (1g) and (1h) respectively. Bus real and reactive power balance constraints in the base case are defined by (1i) and (1j) respectively. The base case line current rating at the origin bus is represented by (1k). The power ratings for the transformer in the base case at the origin bus are shown in (1l).

$$\begin{aligned} \min \sum_{g \in \mathcal{G}} c_g + \frac{1}{|K|} \sum_{k \in \mathcal{K}} \left( \sum_i g(\sigma_{ik}^{P+}, \sigma_{ik}^{P-}, \sigma_{ik}^{Q+}, \sigma_{ik}^{Q-}) \right. \\ \left. + \sum_{e \in \mathcal{E}} h_1(\sigma_{ek}) + \sum_{f \in \mathcal{F}} h_2(\sigma_{fk}) \right) \end{aligned} \quad (1a)$$

**subject to:**

$$\underline{v}_i \leq v_i \leq \bar{v}_i \quad \forall i \in \mathcal{I} \quad (1b)$$

$$\underline{p}_g \leq p_g \leq \bar{p}_g \quad \forall g \in \mathcal{G} \quad (1c)$$

$$\underline{q}_g \leq q_g \leq \bar{q}_g \quad \forall g \in \mathcal{G} \quad (1d)$$

$$\begin{aligned} p_e^{ij} = g_e(e_i^2 + f_i^2) - g_e(e_i e_j + f_i f_j) \\ - b_e(e_i f_j - e_j f_i) \quad \forall e \in \mathcal{E} \end{aligned} \quad (1e)$$

$$\begin{aligned} q_e^{ij} = -(b_e + b_e^{CH}/2)(e_i^2 + f_i^2) + b_e(e_i e_j + f_i f_j) \\ - g_e(e_i f_j - e_j f_i) \quad \forall e \in \mathcal{E} \end{aligned} \quad (1f)$$

$$\begin{aligned} p_f^{ij} = (g_f/\tau_f^2 + g_f^M)(e_i^2 + f_i^2) - g_f/\tau_f(e_i e_j + f_i f_j) \\ - b_f/\tau_f(e_i f_j - e_j f_i) \quad \forall f \in \mathcal{F} \end{aligned} \quad (1g)$$

$$\begin{aligned} q_f^{ij} = (b_f/\tau_f^2 + b_f^M)(e_i^2 + f_i^2) + b_f/\tau_f(e_i e_j + f_i f_j) \\ - g_f/\tau_f(e_i f_j - e_j f_i) \quad \forall f \in \mathcal{F} \end{aligned} \quad (1h)$$

$$\begin{aligned} \sum_{g \in G_i} p_g - p_i^L - g_i^{FS} v_i^2 - \sum_{j \in \delta(i)} p_e^{ij} - \sum_{j \in \psi(i)} p_f^{ij} = 0 \\ \forall i \in \mathcal{I} \end{aligned} \quad (1i)$$

$$\begin{aligned} \sum_{g \in G_i} q_g - q_i^L - b_i^{FS} v_i^2 - \sum_{j \in \delta(i)} q_e^{ij} - \sum_{j \in \psi(i)} q_f^{ij} = 0 \\ \forall i \in \mathcal{I} \end{aligned} \quad (1j)$$

$$\sqrt{(p_e^{ij})^2 + (q_e^{ij})^2} \leq \bar{R}_e \quad \forall e \in \mathcal{E} \quad (1k)$$

$$\sqrt{(p_f^{ij})^2 + (q_f^{ij})^2} \leq \bar{s}_f \quad \forall f \in \mathcal{F} \quad (1l)$$

The constraints associated with each contingency are given in (2). For each contingency, bounds on voltage, real power and reactive power are represented by (2a), (2b), and (2d) respectively. The constraints (2c) and (2e) enforce the real and reactive power of generators that are not active during contingency to zero. The real and reactive power flow into a transmission line at the origin bus during a contingency are defined by (2f) and (2g) respectively. The real and reactive power flow into a transformer at the origin buses in each contingency are shown by (2h) and (2i) respectively. Bus real and reactive power balance constraints during a contingency along with soft constraint violation variables are represented by (2j) and (2l) respectively. The constraints (2k) and (2m) define that soft-constraint violation variables are positive. During each contingency, the line current rating at the origin bus with violation variable ( $\sigma_{ek}$ ) is represented by (2n) and (2o). The transformer power ratings during a contingency at the origin bus along with constraint violation variables are shown in (2p) and (2q). The constraint (2r) shows that an online generator but not selected to respond to contingency, retains its real output power from base case.

$$\underline{v}_i^K \leq v_{ik} \leq \bar{v}_i^K \quad \forall k \in \mathcal{K}, i \in \mathcal{I} \quad (2a)$$

$$\underline{p}_g \leq p_{gk} \leq \bar{p}_g \quad \forall k \in \mathcal{K}, g \in \mathcal{G}_k \quad (2b)$$

$$p_{gk} = 0 \quad \forall k \in \mathcal{K}, g \in \mathcal{G} \setminus \mathcal{G}_k \quad (2c)$$

$$\underline{q}_g \leq q_{gk} \leq \bar{q}_g \quad \forall k \in \mathcal{K}, g \in \mathcal{G}_k \quad (2d)$$

$$q_{gk} = 0 \quad \forall k \in \mathcal{K}, g \in \mathcal{G} \setminus \mathcal{G}_k \quad (2e)$$

$$\begin{aligned} p_{ek}^{ij} = g_e(e_{ik}^2 + f_{ik}^2) - g_e(e_{ik} e_{jk} + f_{ik} f_{jk}) \\ - b_e(e_{ik} f_{jk} - e_{jk} f_{ik}) \quad \forall k \in \mathcal{K}, e \in \mathcal{E} \end{aligned} \quad (2f)$$

$$\begin{aligned} q_{ek}^{ij} = -(b_e + b_e^{CH}/2)(e_{ik}^2 + f_{ik}^2) + b_e(e_{ik} e_{jk} + f_{ik} f_{jk}) \\ - g_e(e_{ik} f_{jk} - e_{jk} f_{ik}) \quad \forall k \in \mathcal{K}, e \in \mathcal{E}_k \end{aligned} \quad (2g)$$

$$p_{fk}^{ij} = (g_f/\tau_f^2 + g_f^M)(e_{ik}^2 + f_{ik}^2) - g_f/\tau_f(e_{ik} e_{jk} + f_{ik} f_{jk})$$

$$-b_f/\tau_f(e_{ik}f_{jk} - e_{jk}f_{ik}) \quad \forall k \in \mathcal{K}, f \in \mathcal{F}_k \quad (2h)$$

$$\begin{aligned} q_{fk}^{ij} &= (b_f/\tau_f^2 + b_f^M)(e_{ik}^2 + f_{ik}^2) + b_f/\tau_f(e_{ik}e_{jk} + f_{ik}f_{jk}) \\ &\quad - g_f/\tau_f(e_{ik}f_{jk} - e_{jk}f_{ik}) \quad \forall k \in \mathcal{K}, f \in \mathcal{F}_k \end{aligned} \quad (2i)$$

$$\begin{aligned} \sum_{g \in G_{ik}} p_{gk} - p_i^L - g_i^{FS}v_{ik}^2 - \sum_{j \in \delta_k(i)} p_{ek}^{ij} \\ - \sum_{j \in \psi_k(i)} p_{fk}^{ij} = \sigma_{ik}^{P+} - \sigma_{ik}^{P-} \quad \forall k \in \mathcal{K}, i \in \mathcal{I} \end{aligned} \quad (2j)$$

$$\sigma_{ik}^{\rho} \geq 0 \quad \forall k \in \mathcal{K}, i \in \mathcal{I}, \rho = \{\mathcal{P}\pm\} \quad (2k)$$

$$\begin{aligned} \sum_{g \in G_{ik}} q_{gk} - q_i^L + b_i^{FS}v_{ik}^2 - \sum_{j \in \delta_k(i)} q_{ek}^{ij} \\ - \sum_{j \in \psi_k(i)} q_{fk}^{ij} = \sigma_{ik}^{Q+} - \sigma_{ik}^{Q-} \quad \forall k \in \mathcal{K}, i \in \mathcal{I} \end{aligned} \quad (2l)$$

$$\sigma_{ik}^{\rho} \geq 0 \quad \forall k \in \mathcal{K}, i \in \mathcal{I}, \rho = \{Q\pm\} \quad (2m)$$

$$\sqrt{(p_{ek}^{ij})^2 + (q_{ek}^{ij})^2} \leq \bar{R}_e^K + \sigma_{ek}^S \quad \forall k \in \mathcal{K}, e \in \mathcal{E}_k \quad (2n)$$

$$\sigma_{ek}^S \geq 0 \quad \forall k \in \mathcal{K}, e \in \mathcal{E}_k \quad (2o)$$

$$\sqrt{(p_{fk}^{ij})^2 + (q_{fk}^{ij})^2} \leq \bar{s}_f^K + \sigma_{fk}^S \quad \forall k \in \mathcal{K}, f \in \mathcal{F}_k \quad (2p)$$

$$\sigma_{fk}^S \geq 0 \quad \forall k \in \mathcal{K}, f \in \mathcal{F}_k \quad (2q)$$

$$p_{gk} = p_g \quad \forall k \in \mathcal{K}, g \in \mathcal{G}_k \setminus \mathcal{G}_P \quad (2r)$$

The constraints presented in (2) do not cover the real and reactive power dispatch of generators participating in the contingency response. The real power ( $p_{gk}$ ) of generator in a contingency  $k$  is governed by the constraints given in (3) [27]. Here, each generator has a pre-defined response rate given by  $\alpha_g$  which is a portion of the total response given in  $\Delta_k$  for the contingency  $k$ . This set of constraints represents the AGC response of the active generation units in the contingency, where the dispatch of generation units during the contingency  $k$  is determined. If the determined value is outside of the physical limits of a generation unit, the dispatch is set to the physical limit and the AGC response is overwritten. The reactive power is subject to the constraints given in (4) [27], the voltage of buses with a generation bus is preserved to the values before the contingency if the reactive power limits are not reached.

$$\left. \begin{aligned} \{p_g \leq p_{gk} \leq \bar{p}_g \quad \& \quad p_{gk} = p_g + \alpha_g \Delta_k\} \\ \{p_{gk} = \bar{p}_g \quad \& \quad p_{gk} \leq p_g + \alpha_g \Delta_k\} \\ \{p_{gk} = \underline{p}_g \quad \& \quad p_{gk} \geq p_g + \alpha_g \Delta_k\} \end{aligned} \right\} k \in \mathcal{K}, g \in \mathcal{G}_k^P \quad (3)$$

$$\left. \begin{aligned} \{\underline{q}_g \leq q_{gk} \leq \bar{q}_g \quad \& \quad \sqrt{e_{i_g k}^2 + f_{i_g k}^2} = \sqrt{e_{i_g}^2 + f_{i_g}^2}\} \\ \{q_{gk} = \bar{q}_g \quad \& \quad \sqrt{e_{i_g k}^2 + f_{i_g k}^2} \leq \sqrt{e_{i_g}^2 + f_{i_g}^2}\} \\ \{q_{gk} = \underline{q}_g \quad \& \quad \sqrt{e_{i_g k}^2 + f_{i_g k}^2} \geq \sqrt{e_{i_g}^2 + f_{i_g}^2}\} \end{aligned} \right\} k \in \mathcal{K}, g \in \mathcal{G}_k \quad (4)$$

In other words, these constraints represent the voltage control of the generation bus. If the upper limits of the reactive power generation are reached, the voltage on the connected bus is equal lower than that before the contingency. If the lower limits of the reactive power generation are reached, the voltage on the connected bus is equal greater than that before the

contingency. The presented constraints in (3) and (4) are not straightforward to model in an optimization problem and will generally require employment of binary variables which cause an increase in the computation burden of each sub-problem. A set of valid constraints are introduced in the next section to solve the problem without employing binary variables.

### III. SOLUTION METHOD

The problem presented in section II has three issues. First, the problem is nonlinear and non-convex. Thus, it is challenging to solve. Therefore, a convex relaxation technique is presented in subsection III-A to address this challenge. Second, the presented set of constraints in (3) and (4) are non-linear and cannot be directly incorporated into the AC-OPF problem formulation. Thus, a set of valid constraints are introduced in subsection III-B to resolve this problem. Third, the set of contingencies dramatically increases the size of the problem. To address this challenge, a decomposition method is employed and it is discussed in subsection III-C.

#### A. Formulating the Base Case Problem as a Second-Order Convex Relaxation

The base case problem presented in (1) is a non-convex optimization problem. The non-convexity arises because of the expressions  $e_i^2 + f_i^2$ ,  $e_i e_j + f_i f_j$ , and  $e_i f_j - e_j f_i$ . To convexify the problem, new variables are defined as  $c_{ii} := e_i^2 + f_i^2$ ,  $c_{ij} := e_i e_j + f_i f_j$  and  $s_{ij} := e_i f_j - e_j f_i$ . The revised base problem formulation is given in (5). Base case real and reactive power flow into a transmission line at the origin buses from (1e) and (1f) are updated to (5b) and (5c) respectively. The real and reactive power flow into a transformer at the origin buses in the base case from (1g) and (1h) are revised to (5d) and (5e) respectively. The complex voltage magnitude at bus  $i$  is restricted by the constraint (5f). The characteristics of  $c_{ij}$  and  $s_{ij}$  are given in (5g) and these new variables satisfy the relationship in (5h) which is a second-order cone constraint. The base case problem is now convex and can be solved using off-the-shelf solvers.

$$\min \sum_{g \in G} c_g + \delta c^\sigma \quad (5a)$$

**subject to:**

$$(1b) - (1d)$$

$$p_e^{ij} = g_e c_{ii} - g_e c_{ij} - b_e s_{ij} \quad \forall e \in \mathcal{E} \quad (5b)$$

$$q_e^{ij} = -(b_e + b_e^{CH}/2)c_{ii} + b_e c_{ij} - g_e s_{ij} \quad \forall e \in \mathcal{E} \quad (5c)$$

$$\begin{aligned} p_f^{ij} &= (g_e + g_{ii})/t_m^2 c_{ii} + (-g_e t_r + b_e t_i)/t_m^2 c_{ij} \\ &\quad + (-b_e t_r - g_e t_i)/t_m^2 s_{ij} \quad \forall f \in \mathcal{F}, e \in \mathcal{E} \end{aligned} \quad (5d)$$

$$\begin{aligned} q_f^{ij} &= -(b_e + b_{ii})/t_m^2 c_{ii} - (-b_e t_r - g_e t_i)/t_m^2 c_{ij} \\ &\quad + (-g_e t_r + b_e t_i)/t_m^2 s_{ij} \quad \forall f \in \mathcal{F}, e \in \mathcal{E} \end{aligned} \quad (5e)$$

$$(1i) - (1l)$$

$$\underline{v}_i^2 \leq c_{ii} \leq \bar{v}_i^2 \quad i \in \mathcal{I} \quad (5f)$$

$$c_{ij} = c_{ji}, \quad s_{ij} = -s_{ji} \quad (i, j) \in \mathcal{E} \quad (5g)$$

$$c_{ij}^2 + s_{ij}^2 \leq c_{ii} c_{jj} \quad (i, j) \in \mathcal{E} \quad (5h)$$

The tightness of the procured solution obtained from convex relaxation is measured by taking the difference between  $c_{ij}^2 +$

$s_{ij}^2$  and  $c_{ii}c_{jj}$ . In an ideal scenario, the difference is zero and it means that the relaxation is exact. Nevertheless, in practice, the difference exists. The quality of the solution is determined by measuring how far the difference is from zero. The negative logarithmic of the difference is taken due to the small value. Thus, the mathematical representation of tightness measure ( $T$ ) is given in (6).

$$T_{ij} = -\log|c_{ij}^2 + s_{ij}^2 - c_{ii}c_{jj}| \quad (6)$$

### B. Modeling AGC Response

This section addresses the generator real power contingency (3) and reactive power contingency (4) responses. Recurrent changes to the output of a power generator are necessary because the generated power and load should be balanced during a contingency in the power system. A set of valid constraints are presented in (7) for modeling the AGC response during a contingency.

$$(2a) - (2r)$$

$$(p_{gk} - (p_g + \alpha_g \Delta_k))(p_{gk} - \bar{p}_g) \leq 0 \quad \forall k \in \mathcal{K}, g \in \mathcal{G}_k^P \quad (7a)$$

$$(p_{gk} - (p_g + \alpha_g \Delta_k))(\underline{p}_g - p_{gk}) \geq 0 \quad \forall k \in \mathcal{K}, g \in \mathcal{G}_k^P \quad (7b)$$

$$((e_{i_g}^2 + f_{i_g}^2) - (e_{i_g k}^2 + f_{i_g k}^2))(q_{gk} - \bar{q}_g) \geq 0 \quad \forall k \in \mathcal{K}, \\ g \in \mathcal{G}_k^P \quad (7c)$$

$$((e_{i_g k}^2 + f_{i_g k}^2) - (e_{i_g}^2 + f_{i_g}^2))(\underline{q}_g - q_{gk}) \geq 0 \quad \forall k \in \mathcal{K}, \\ g \in \mathcal{G}_k^P \quad (7d)$$

The generator real power contingency response presented in (3) is updated to (7a) and (7b). If the real power generation dispatch is in an open interval within the generation limits, the dispatch is determined using the participation factor and system wide changes of each contingency i.e. LHS of constraints (7a) and (7b) are both zero. If the real power generation dispatch hits the physical limits, the dispatch is equal to the physical limit and is not based on the participation factor and base case power dispatch. If the upper limits reached, LHS of (7a) is zero and the second term on the LHS of (7b) is negative, so its first term should be smaller than or equal to zero i.e. the actual dispatch being equal or smaller than the desired one determined by the participation factor. Similarly, if the lower limits reached, LHS of (7b) is zero and the second term on the LHS of (7a) is negative, so its first term should be greater than or equal to zero i.e. the actual dispatch being equal or greater than the desired one is determined by the participation factor.

Moreover, reactive power contingency response presented in (4) is revised to (7c) and (7d). The voltage of buses with a generator connected to them is equal to the base case voltage during a contingency if the reactive power dispatch of that generator is within an open interval of its physical limits, where the LHS of (7c) and (7d) are zero. If the upper limits of the reactive power dispatch is reached, LHS of (7c) is zero and the second term on the LHS of (7d) is negative, so its first term should be smaller than or equal to zero i.e. the generation bus voltage during the contingency is equal or smaller than the that of the base case. Similarly, if the lower limits of the reactive power dispatch reached, LHS

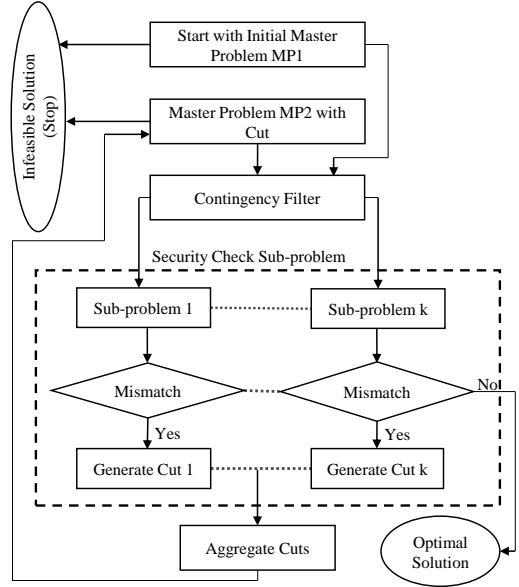


Fig. 1. Flowchart of Benders Decomposition

of (7d) is zero and the second term on the LHS of (7c) is negative, so its first term should be smaller than or equal to zero i.e. the generation bus voltage during the contingency is equal or greater than the that of the base case. Thus, the procured constraints represent a set of valid constraints that can be integrated into the SCOPF problem formulation without introducing any binary variables. Employing these constraints will significantly reduce the computation time for the AGC response in the SCOPF calculations as demonstrated in the case studies.

### C. Problem Decomposition

To enable solving large-scale optimization problems, Benders decomposition is implemented and it is described in this subsection. The flowchart of the Benders decomposition is given in Fig. 1.

- 1) Solve the initial master problem MP1 using the convex relaxation method presented in subsection III-A. Obtain the lower bound ( $z_{lower}$ ) for the objective value. If MP1 is infeasible, the original problem is infeasible. The abstract formulation of the master problem is given in (8).

$$\min_{x \in \mathcal{X}, v \in \mathcal{V}} c^T x \quad (8a)$$

$$s.t. \quad Ax + Bv = d \quad (8b)$$

$$Cx + Dv \leq e \quad (8c)$$

The equality constraint (8b) represents the equality constraints in (5) and the inequality constraint (8c) represents the inequality constraints in (5).

- 2) Apply the contingency filtering technique to build a static ordering of all contingencies. The procured contingency filter ranks the components based on their significance in terms of utilization in the system. Thus, the contingencies that lead to the largest constraint violations are selected using the procured mismatches and a Benders cut for each violated contingency is added



Fig. 2. A sample donut chart of parallel computation process with 6 workers and three levels of filtering.

to the master problem. Three levels of filters are applied as shown in Fig. 2, where Filter 1 represents the most critical contingencies.

3) Pass the master problem solution to each sub-problem and solve it in a parallel computing process. The parallel computation technique accelerates the sub-problems solution because it involves multiple workers solving the security check sub-problems. It offers an environment that applies message passing interface to allow multiple workers to solve contingencies in a distributed memory. Each worker has its own private memory in a distributed memory environment. Message passing interface is a form of communication used in parallel computation that helps different workers to communicate with each other. In the proposed algorithm, there is one master worker and workers  $1, \dots, n$ , e.g.  $n = 6$  in Fig. 2. The workers  $1, \dots, n$  point their nodes towards the master worker. The master worker sends functions, data packets and signals to workers  $1, \dots, n$  using message passing interface. The filtered contingencies are distributed among the available workers by dividing the total number of contingencies and the workers. Finally, the workers return  $z_{upper}$  of the objective value for each sub-problem in the array. The abstract composition of sub-problem is given in (9).

$$\min_{x_k \in \mathcal{X}, v_k \in \mathcal{V}} f(\sigma) \quad (9a)$$

$$s.t. \quad F_k(\mathbf{x}_k, \mathbf{v}_k, \sigma_k) = 0 \quad : \lambda_k \quad (9b)$$

$$G_k(\mathbf{x}_k, \mathbf{v}_k) \geq 0 \quad : \mu_k \quad (9c)$$

The subproblem objective is to minimize the mismatches. The equality constraint (9b) represents the equality constraints in (7) and the inequality constraint (9c) represents the inequality constraints in (7).

The Benders cut for the master problem is given in (10).

$$z_{lower} \geq d^T y + (h - Fy)^T \hat{u}^p \quad (10)$$

4) Obtain the upper bound ( $z_{upper}$ ) of the objective value from sub-problems solution. Check the mismatch between  $z_{upper}$  and  $z_{lower}$ . If there is no mismatch, the

optimal solution is procured. Otherwise, continue to the next step.

- 5) For each sub-problem, a Benders cut is generated. The cuts are aggregated and applied to the master problem MP2 with cuts.
- 6) Repeat steps 3-5 until the total mismatch is less than a desired threshold.

#### IV. CASE STUDY

In this section, three case studies are presented to demonstrate the effectiveness of the proposed algorithm for security-constrained AC-OPF. The first case study uses IEEE 14-bus system, the second uses 500-bus system, and the third uses 2000-bus system. The case studies are performed on a standard PC with an Intel Core i7-9700K CPU running at 3.60 GHz and 16.0 GB RAM. Julia built-in PMAP function is used for solving the sub-problems in parallel. PMAP applies the sub-problem constraints concurrently to the contingencies present in the array.

##### A. IEEE 14-Bus Power System

In this case, a 14-bus power system, which consists of 14 buses, 5 generating units and 11 loads is deployed. This network contains 2 contingency scenarios where the outages occur on the branch connected between bus 6 and 12 and the least utilized generator 5 connected to bus 8. First, the master problem during the normal operating conditions is solved and the voltages at each bus are recorded as shown in column  $v_i$  of Table I corresponding to each bus index  $i$ . For contingency scenario, the branch is taken out of system and the power flow is performed to identify the mismatches. The voltages during the branch contingency at each bus are shown by  $v_{i1}$ . For the case of least utilized generator contingency, the voltages are shown in column  $v_{i2}$ . The voltages of bus 1 for each contingency stays the same because it is a PV bus. This indicates the success of the presented solution method to preserve the voltage-controlled buses. The only exception is the voltage of bus 8 which is permitted to variate because the contingent generator is connected to it. The generator index column indicates the connection of each generator to the particular bus.

TABLE I  
BUS VOLTAGES DURING BASE AND CONTINGENCY CASES

Bus Index ( $i$ )	$v_i$	$v_{i1}$	$v_{i2}$	Generator Index
1	<b>1.098</b>	<b>1.098</b>	<b>1.098</b>	1
2	1.093	1.093	1.093	2
3	1.068	1.068	1.068	3
4	1.071	1.071	1.069	-
5	1.076	1.074	1.073	-
6	1.099	1.099	1.099	4
7	1.095	1.089	1.080	-
8	<b>1.099</b>	<b>1.099</b>	<b>1.080</b>	5
9	1.093	1.079	1.073	-
10	1.087	1.074	1.069	-
11	1.090	1.081	1.079	-
12	1.087	1.058	1.086	-
13	1.083	1.073	1.079	-
14	1.073	1.060	1.059	-

Table II shows the automatic generation control response during each contingency. For the branch contingency, the real power generation  $p_{g1}$  from generators 1 – 3 and 5 is increased while it is the same for generator 4 because it was hitting the upper limit during the normal operating conditions. This indicates the success of the presented reformulation in preserving the AGC response of generation units under contingency. The reactive power  $q_{g1}$  for generators 1, 3 and 5 is increased while it is decreased for 2 and 4. As these reactive power values are within the limits of each generation unit, it is consistent with the voltage value presented in Table I. When the least utilized generator 5 is under contingency, the real and reactive powers from it are zero. In this case, the real power  $p_{g2}$  for generators 1 – 3 is increased while it is the same for generator 4 because it reached the maximum limit. The reactive power  $q_{g2}$  is increased for generators 1 – 3 while it is decreased for generator 4. The minimum and maximum values of real and reactive power, as well as the participation factors for each generation unit, are shown in Table II. The value of  $\Delta_1$  is 0.02 MW for branch contingency and the value of  $\Delta_2$  is -0.106 MW for generator contingency.

The tightness measure of the procured solution obtained from

TABLE II  
AUTOMATIC GENERATION CONTROL RESPONSE DURING A  
CONTINGENCY

Generator Index	1	2	3	4	5
$p_g$	37.96	83.29	5.80	<b>110.50</b>	0.32
$q_g$	1.84	18.69	27.62	-4.98	2.85
$p_{g1}$	38.07	83.67	6.79	<b>110.50</b>	0.38
$q_{g1}$	<b>2.57</b>	17.53	27.86	-14.16	<b>6.70</b>
$p_{g2}$	38.08	83.71	6.91	<b>110.50</b>	0
$q_{g2}$	<b>3.16</b>	19.41	29.00	-11.40	0
$p_{min}$	37.96	48.15	5.80	11.46	0.32
$p_{max}$	245.45	157.50	82.50	<b>110.50</b>	80.14
$q_{min}$	<b>-132.20</b>	-76.98	-0.88	-19.11	-8.03
$q_{max}$	<b>76.06</b>	36.17	48.51	19.47	19.24
$\alpha$	5	19	49.3	38.8	3

convex relaxation is determined using (6) and tabulated in Table III. The gap between the proposed solution and the original problem is very small because the logarithmic value of the tightness is in-between 7 and 10. Thus, the tightness of the procured relaxation scheme represents that the proposed scheme is very close to the original one and a good quality solution is obtained.

TABLE III  
TIGHTNESS MEASURE OF BUS-PAIRS OF THE IEEE 14-BUS SYSTEM

Bus-pair	$T_{ij}$	Bus-pair	$T_{ij}$	Bus-pair	$T_{ij}$
(1,2)	8.0012	(6,11)	7.7436	(5,6)	8.1014
(1,5)	8.0060	(6,12)	7.7453	(13,14)	8.0052
(2,3)	8.0053	(6,13)	7.7453	(4,9)	7.7431
(2,4)	8.0036	(7,8)	7.6488	(12,13)	8.0024
(2,5)	8.0036	(7,9)	8.7622	(4,7)	9.8836
(3,4)	8.0029	(9,10)	8.0015	(10,11)	8.0032
(4,5)	8.0008	(9,14)	8.0042		

### B. 500-Bus Power System

In this case, a 500-bus power system is utilized consisting of 90 generators, 200 loads and 131 transformers. It consists of 51 transformer contingencies and 326 branch contingencies. Table IV shows the results when the contingency filter is 0.5,

which means that the top critical 50% of total contingencies are taken into account. The master problem objective value is written in 0<sup>th</sup> iteration. With each iteration, the number of sub-problem contingencies that violated the rating decreases due to the Benders cuts applied to the master problem. An updated value of the objective is obtained after applying the cuts to the master problem. The objective value is increased from \$27,529 to \$73,491 in 9 iterations. The total mismatch for the contingencies decreases sharply with each iteration. The mismatch in 2<sup>nd</sup> iteration (21,379) is less than one half the value in 1<sup>st</sup> iteration (53,192). The algorithm converges in 9<sup>th</sup> iteration with 0 mismatch.

TABLE IV  
SUMMARY OF RESULTS FOR 500-BUS SYSTEM

Iterations [n]	Violations	Objective [\$]	Mismatch
0	-	27,529.7	-
1	188	73,491.5	53,192.4
2	93	73,491.5	21,379.8
3	46	73,491.5	9,164.1
4	22	73,491.5	4,812.1
5	11	73,491.5	2,379.3
6	5	73,491.5	937.8
7	2	73,491.5	362.0
8	1	73,491.5	170.5
9	0	73,491.5	0

By selecting critical contingencies active in the 500-bus power system, the effect on objective, the number of iterations, and the parallel (Par. Time) versus non-parallel (Series Time) solution convergence time of contingencies is tabulated in Table V. The percentage of active contingencies is decreased from 99% to  $N - 1$ . When 99% contingencies are active, the solution is converged in 188 iterations and convergence time is 58,874 seconds for parallel contingency solution case and very large for the non-parallel contingency solution case. For  $N - 1$  contingency scenario, the solution is converged in 3 iterations and it took 183 seconds for the parallel and 494 seconds for the non-parallel situations. The merit of the parallel computation is that it solves the sub-problems on average of 18 times faster. For non-parallel cases, the computation time becomes infinitely large when large set of contingencies are evaluated. Thus, the contingency filtering technique ensures the security check of the procured AC-OPF solution by only considering the critical contingencies and the parallel computation approach make that happen in a time efficient way.

TABLE V  
DIFFERENT CONTINGENCY FILTERS TO OBSERVE THE EFFECT ON  
OBJECTIVE VALUE, ITERATIONS AND SOLUTION CONVERGENCE TIME

Filter	Obj. [\$]	Iters.	Par. Time [s]	Series Time [s]
0.01	131,234.2	188	58,874	N/A
0.25	93,796.6	18	4,941	139,015
0.5	73,491.5	9	2,123	46,814
0.75	45,849.1	5	765	16,053
0.99	28,333.5	3	183	494

### C. 2000-Bus Power System

To demonstrate the efficiency of the proposed algorithm on a large power system network, a 2000-bus power system is considered. It consists of 544 generators, 1,125 loads,

and 847 transformers. There are 432 generator contingencies and 2,753 branch contingencies summing to 3,185. In this case, top 10% of critical contingencies are considered. The mismatch, objective value, and contingencies that violated the power limits for each iteration are tabulated in Table VI. The master problem objective value is \$741,696. During the first iteration, the objective value is increased to \$964,912 and the contingencies that violated the limits are 320. The value of mismatch is decreased sharply from 352,940 to 0 in 5 iterations. The effectiveness of the proposed algorithm can be validated from the fact that after 1<sup>st</sup> iteration, the violated contingencies decreased from 320 to 33 and mismatch reduced from 352,940 to 35,858. The algorithm is capable of solving critical contingencies from large number of contingencies in a time efficient way. Thus, the presented algorithm is computationally efficient for a large network with potential contingencies.

TABLE VI  
SUMMARY OF RESULTS FOR 2000-BUS SYSTEM

Iterations [n]	Violations	Objective [\$]	Mismatch
0	-	741,696.3	-
1	320	964,912.7	352,940.7
2	33	964,912.7	35,858.7
3	3	964,912.7	3,291.1
4	1	964,912.7	936.9
5	0	964,912.7	0

## V. CONCLUSION

This paper proposed a reformulation for the AGC formulation in a decomposed convex relaxation algorithm to find an optimal solution to the AC-OPF problem which is secure against a large number of contingencies. The master problem is convexified by the second-order cone relaxation technique. The contingencies are filtered based on the component utilization factor for corrective or preventive action. The parallel computing process is used to assess the contingencies for preventive security check sub-problems and it ensures the computational efficiency. The automatic generation control response of generating units modeled by valid constraints represents that the solution obtained in each security check sub-problem is the physical response of the system during contingency. Each sub-problem mismatch is addressed by adding a Benders optimally cut to the master problem. The convexified master problem assures the convergence of the decomposition algorithm. Several case studies are presented to demonstrate the competence of the proposed valid AGC constraints and the scalability of the presented algorithm for the security-constrained optimal power flow problem.

## REFERENCES

- [1] A. J. Wood, B. F. Wollenberg, and G. B. Sheblé, *Power generation, operation, and control*. John Wiley & Sons, 2013.
- [2] O. Alsac and B. Stott, "Optimal load flow with steady-state security," *IEEE transactions on power apparatus and systems*, no. 3, pp. 745–751, 1974.
- [3] A. Monticelli, M. Pereira, and S. Granville, "Security-constrained optimal power flow with post-contingency corrective rescheduling," *IEEE Transactions on Power Systems*, vol. 2, no. 1, pp. 175–180, 1987.
- [4] F. Capitanescu and L. Wehenkel, "A new iterative approach to the corrective security-constrained optimal power flow problem," *IEEE transactions on power systems*, vol. 23, no. 4, pp. 1533–1541, 2008.
- [5] T. B. Nguyen and M. Pai, "Dynamic security-constrained rescheduling of power systems using trajectory sensitivities," *IEEE Transactions on Power Systems*, vol. 18, no. 2, pp. 848–854, 2003.
- [6] Y. Fu, M. Shahidehpour, and Z. Li, "AC contingency dispatch based on security-constrained unit commitment," *IEEE Transactions on Power Systems*, vol. 21, no. 2, pp. 897–908, 2006.
- [7] X. Wu, A. J. Conejo, and N. Amjady, "Robust security constrained ACOPF via conic programming: Identifying the worst contingencies," *IEEE Transactions on Power Systems*, vol. 33, no. 6, pp. 5884–5891, 2018.
- [8] F. Capitanescu, J. M. Ramos, P. Panciatici, D. Kirschen, A. M. Marcolini, L. Platbrood, and L. Wehenkel, "State-of-the-art, challenges, and future trends in security constrained optimal power flow," *Electric Power Systems Research*, vol. 81, no. 8, pp. 1731–1741, 2011.
- [9] I. Konstantelos, G. Jamgotchian, S. H. Tindemans, P. Duchesne, S. Cole, C. Merckx, G. Strbac, and P. Panciatici, "Implementation of a massively parallel dynamic security assessment platform for large-scale grids," *IEEE Transactions on Smart Grid*, vol. 8, no. 3, pp. 1417–1426, 2016.
- [10] D.-H. Kuo and A. Bose, "A generation rescheduling method to increase the dynamic security of power systems," *IEEE Transactions on Power Systems*, vol. 10, no. 1, pp. 68–76, 1995.
- [11] C. Wang, B. Cui, Z. Wang, and C. Gu, "SDP-based optimal power flow with steady-state voltage stability constraints," *IEEE Transactions on Smart Grid*, vol. 10, no. 4, pp. 4637–4647, 2018.
- [12] J. Gunda, G. P. Harrison, and S. Z. Djokic, "Remedial actions for security constraint management of overstressed power systems," *IEEE Transactions on Power Systems*, vol. 33, no. 5, pp. 5183–5193, 2018.
- [13] B. Cui and X. A. Sun, "A new voltage stability-constrained optimal power-flow model: Sufficient condition, socp representation, and relaxation," *IEEE Transactions on Power Systems*, vol. 33, no. 5, pp. 5092–5102, 2018.
- [14] B. Park, J. Holzer, and C. L. DeMarco, "A sparse tableau formulation for node-breaker representations in security-constrained optimal power flow," *IEEE Transactions on Power Systems*, vol. 34, no. 1, pp. 637–647, 2018.
- [15] F. Capitanescu, M. Glavic, D. Ernst, and L. Wehenkel, "Contingency filtering techniques for preventive security-constrained optimal power flow," *IEEE Transactions on Power Systems*, vol. 22, no. 4, pp. 1690–1697, 2007.
- [16] G. Ejebé and B. F. Wollenberg, "Automatic contingency selection," *IEEE transactions on Power Apparatus and Systems*, no. 1, pp. 97–109, 1979.
- [17] F. Karbalaei, H. Shahbazi, and M. Mahdavi, "A new method for solving preventive security-constrained optimal power flow based on linear network compression," *International Journal of Electrical Power & Energy Systems*, vol. 96, pp. 23–29, 2018.
- [18] O. Obadina and G. Berg, "VAR planning for power system security," *IEEE Transactions on Power Systems*, vol. 4, no. 2, pp. 677–686, 1989.
- [19] Y. Li and J. D. McCalley, "Decomposed SCOPF for improving efficiency," *IEEE Transactions on Power Systems*, vol. 24, no. 1, pp. 494–495, 2008.
- [20] M. Shahidehpour and Y. Fu, "Benders decomposition: applying benders decomposition to power systems," *IEEE Power and Energy Magazine*, vol. 3, no. 2, pp. 20–21, 2005.
- [21] J. Martínez-Crespo, J. Usaola, and J. L. Fernández, "Security-constrained optimal generation scheduling in large-scale power systems," *IEEE Transactions on Power Systems*, vol. 21, no. 1, pp. 321–332, 2006.
- [22] N. Li, C. Zhao, and L. Chen, "Connecting automatic generation control and economic dispatch from an optimization view," *IEEE Transactions on Control of Network Systems*, vol. 3, no. 3, pp. 254–264, 2015.
- [23] E. Mallada, C. Zhao, and S. Low, "Optimal load-side control for frequency regulation in smart grids," *IEEE Transactions on Automatic Control*, vol. 62, no. 12, pp. 6294–6309, 2017.
- [24] M. Vrakopoulou, M. Katsampani, K. Margellos, J. Lygeros, and G. Andersson, "Probabilistic security-constrained AC optimal power flow," in *2013 IEEE Grenoble Conference*. IEEE, 2013, pp. 1–6.
- [25] M. Ni, J. D. McCalley, V. Vittal, and T. Tayyib, "Online risk-based security assessment," *IEEE Transactions on Power Systems*, vol. 18, no. 1, pp. 258–265, 2003.
- [26] A. Street, F. Oliveira, and J. M. Arroyo, "Contingency-constrained unit commitment with  $n - k$  security criterion: A robust optimization approach," *IEEE Transactions on Power Systems*, vol. 26, no. 3, pp. 1581–1590, 2010.
- [27] C. J. Coffrin, "ARPA-E grid optimization competition, SCOPF overview," Los Alamos National Lab.(LANL), Los Alamos, NM (United States), Tech. Rep., 2019.